SCIENTIA AGROPECUARIA

Scientia Agropecuaria

Web page: http://revistas.unitru.edu.pe/index.php/scientiaagrop

Facultad de Ciencias Agropecuarias

Universidad Nacional de Trujillo

RESEARCH ARTICLE

Isosteric heat of sorption in powders produced from agro-industrial byproducts: a systematic review and meta-analysis

Miguel Chamache[1]; Meliza Lindsay Rojas[2]; Guillermo Linares[3]*

[1] Escuela de Ingeniería Agroindustrial, Universidad Nacional de Trujillo, Perú.
[2] Dirección de Investigación, Innovación y Sostenibilidad, Universidad Privada del Norte (UPN), Trujillo, Perú.
[3] Grupo de Investigación "Revalorización de subproductos agroindustriales – REVALORAGRO", Universidad Nacional de Trujillo, Perú.

* Corresponding author: glinares@unitru.edu.pe (G. Linares).

Received: 12 October 2025. Accepted: 4 May 2026. Published: 13 May 2026.

Abstract

This systematic review and meta-analysis aimed to analyze data published since 2007 on the isosteric heat of sorption (q_{st}) in powdered foods derived from agro-industrial by-products, in order to support the optimization of dehydration processes and their sustainable use in the food industry. Twenty-five studies were included following a structured search strategy. Results showed that powdered by-products predominantly exhibit Brunauer type II (sigmoidal) and type III isotherms, strongly influenced by their composition. Type II curves were associated with protein-, starch-, and biopolymer-rich powders, while type III behavior characterized sugar- and fiber-rich matrices. The Guggenheim–Anderson–de Boer (GAB) model consistently provided the best fit ($R^2 > 0.90$), with monolayer moisture content (X_m) ranging from 0.006 to 0.6 g water/g dry matter and generally decreasing with temperature. Cluster analysis grouped powders according to X_m values, composition, and temperature, highlighting the role of matrix structure in water retention behavior. The isosteric heat of sorption (q_{st}) exhibited both endothermic and exothermic behavior (–88.4 to 58.0 kJ/mol), with higher energy requirements during desorption. Principal Component Analysis (PCA) revealed that X_m is mainly associated with fiber-rich matrices, whereas the GAB parameter C is linked to carbohydrate and lipid fractions. In contrast, q_{st} showed weak association with the principal components, indicating that sorption energetics are not directly aligned with structural variability but rather reflect localized molecular interactions. Overall, sorption behavior of powdered by-products is governed by the combined effect of composition, structural water retention, and energetic interactions, which are critical for improving drying and storage conditions.

Keywords: Powder by-products; sorption properties; isosteric heat; principal component analysis; powder properties.

DOI: https://doi.org/10.17268/sci.agropecu.2026.039

Cite this article:

Chamache, M., Rojas, M. L., & Linares, G. (2026). Isosteric heat of sorption in powders produced from agro-industrial byproducts: a systematic review and meta-analysis. *Scientia Agropecuaria, 17*(2), 557-576.

1. Introduction

The valorization of agro-industrial by-products, such as peels, seeds, stalks, and pomace, represents a key strategy for sustainable development, particularly in relation to Sustainable Development Goals (SDGs), among these: SDGs 12 (responsible production and consumption), SDGs 15 (life on land), SDGs 2 (zero hunger), SDGs 7 (affordable &clean energy), SDGs 8 (decent work & economic growth), and SDGs 9 (Industry innovation & infrastructure) (Ahmad et al., 2024). This approach not only reduces the ecological footprint associated with waste disposal but also optimizes resource transforming by-products into value-added products such as powders, which have gained increasing relevance due to their nutritional content and versatility (Panesar et al., 2015). Several studies have demonstrated that agro-industrial by-products can be converted into sustainable sources of functional compounds—such as proteins, antioxidants, and dietary fiber—through technologically feasible processes, thereby reinforcing their potential in the context of food security and environmental sustainability (Piercy et al., 2022; Ray & Boruah, 2024).

In regions with high agricultural and industrial activity, large quantities of food by-products, an estimated 1.3 billion tons each year (including plant fibers, bracts, seeds, bagasse, and peels) are generated during the processing of fruits, vegetables, and other raw materials (Boudalia et al., 2026). However,

many of these by-products remain underutilized for human food applications. Their use is mainly restricted to animal feed or composting, which reveals a missed opportunity for technological innovation, circular economy practices, and full biomass valorization (Balakrishnan et al., 2025). This issue becomes even more critical considering the growing demand for processed foods that combine convenience, nutritional value, and storage stability—characteristics that powders based on by-products can provide while promoting sustainability (Santos et al., 2022).

In recent years, the global consumption of powdered foods has increased significantly, driven by consumer demand for ready-to-use products. In addition, their physicochemical and microbiological stability ensures quality and safety during storage (Ueda et al., 2023). The production of such powders through controlled dehydration techniques has proven effective in producing physically, chemically, and microbiologically stable powders (Duarte et al., 2017; Osorio-Arias et al., 2020), extending shelf life and enhancing their suitability for transport, storage, and integration into food systems. As a result, powders can be reintegrated into both industrial and household settings as sources of functional and technological compounds (Cuq et al., 2011; Hickey & Giovagnoli, 2018; Lisboa et al., 2018; Ramírez-Pulido et al., 2021; Rifna et al., 2019; Ueda et al., 2023). Therefore, powders based on by-products can be used as functional or technological additives, such as colorants, preservatives, thickeners, and carriers of bioactive compounds. However, some important powder properties, such as their thermodynamic properties, are still underexplored.

Thermodynamic properties are essential for determining the final moisture content when food is dehydrated into a powder (Muzaffar & Kumar, 2016). They also play a key role in predicting the minimum amount of energy required for water removal (Arslan & Toğrul, 2006; Goneli et al., 2016). Among these properties, the isosteric heat, enthalpy, entropy, and Gibbs free energy are critical for describing the energy input, molecular order, and reactions involved during sorption processes in food materials. A thorough understanding of these properties is essential for evaluating the stability and quality of powdered foods, particularly those derived from agro-industrial by-products.

Although various reviews have addressed sorption kinetics and isotherm models, most focus on adsorbent properties for industrial applications and often overlook the thermodynamic behavior of powders derived from food by-products. This gap is further complicated by methodological inconsistencies across experimental studies, such as variations in moisture ranges and analytical approaches, which limit comparability and hinder the development of optimized dehydration and storage models. Therefore, systematic reviews and meta-analyses are essential to consolidate and standardize available data. However, the interpretation of sorption behavior remains challenging due to compositional variability and experimental diversity. In this context, multivariate approaches offer a useful framework to better understand the relationships between composition and sorption parameters.

In this context, the information reported in various studies for calculating the isosteric heat of sorption in powdered foods will help identify behavior patterns useful for extending shelf life and reducing energy consumption during processing. The general objective of this research is to describe and analyze data published since 2007 regarding the isosteric heat of sorption in powdered foods produced from agro-industrial by-products. This aims to contribute to the optimization of technological processes related to the dehydration and preservation of these products and to provide scientific evidence for their sustainable use in the food industry.

2. Methodology

2.1 Systematic Review and Meta-analysis Protocol

This study was conducted as a systematic review and meta-analysis focused on the isosteric heat of sorption in food powders produced from agro-industrial byproducts, following the procedures outlined in the methodology (Figure 1).

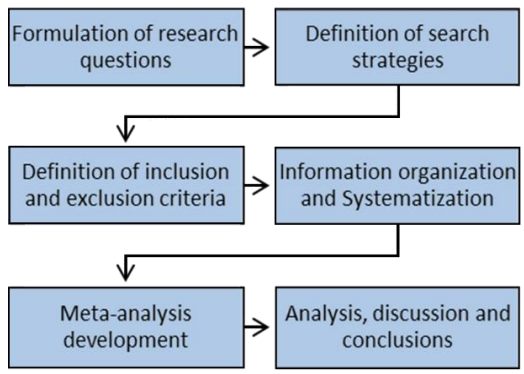

Figure 1. Methodological approach for systematic review and meta-analysis.

2.1.1 Formulation of research questions

For the development of Systematic review and meta-analysis, the research questions (RQs) relevant to the search, extraction, and data analysis strategy were established. For each question, the objectives were also formulated, as shown in Table 1.

Table 1
Research Questions and Objectives

Research Question (RQ)	Objective
RQ1: What types of sorption isotherms are most frequently reported in food powders obtained from agro-industrial residues, and how are they related to the powders' chemical composition (e.g., fiber, starch, protein, sugars)?	Identify the predominant types of sorption isotherms in food powders derived from agro-industrial residues and relate them to the main compositional characteristics of the powders.
RQ2: How do GAB model parameters vary with temperature, composition, and processing conditions, and what moisture ranges ensure the physicochemical stability of food powders from agro-industrial residues?	Evaluate how GAB parameters vary with key factors and identify moisture values that ensure powder stability.
RQ3: What is the typical range and thermal behavior (endothermic or exothermic) of isosteric heat of sorption ($\mathbf{q_{st}}$) in food powders derived from agro-industrial by-products?	Determine the typical range and thermal behavior (endothermic or exothermic) of the isosteric heat of sorption (q_{st}) in food powders derived from agro-industrial by-products.
RQ4: Which compositional factors influence the variability of $\mathbf{q_{st}}$ values among different food powders obtained from agro-industrial by-products?	Analyze the influence of compositional factors—such as protein, starch, lipid, and fiber content—on the variability of q_{st} values across different types of food powders.

2.1.2 Definition of search strategies

Information was searched in Scopus, ScienceDirect, SciELO, and Redalyc. The main reasons for selecting these repositories were to maximize recall and avoid geographic bias, the quality of the research content, their open access to databases, and their recognition and prestige among academic and scientific researchers.

A single search equation was designed to retrieve a broad corpus of articles addressing the topic of isosteric heat of sorption in food powders from agro-industrial by-products. This was chosen since all four research questions (RQ1–RQ4) address different facets of the same set of studies — namely: isotherm type (RQ1), GAB model parameters (RQ2), q_{st} range and thermal behavior (RQ3), and compositional drivers of q_{st} (RQ4). For the search process, keywords and Boolean operators were used (Table 2). The terms were extracted from the keywords of research articles related to the topic of the project and from an exhaustive search in recognized research repositories. In addition, the heterogeneity in search fields across databases was also considered, and the search field used in each database was specified in Table 2.

2.1.3 Selection criteria

To ensure a rigorous assessment of information quality, a set of exclusion criteria (EC) was established. The selection of articles was guided by these specific exclusion criteria. Seven distinct criteria were applied to refine the pool of eligible publications, as detailed below.

EC1: The papers are more than twenty years old
EC2: The papers were not published in peer-reviewed journals or conferences.
EC3: The papers are not written in English or Spanish.
EC4: The papers are not unique (duplicated).
EC5: The reviewed papers are bibliometric reviews or systematic reviews
EC6: The papers do not include powders obtained from residues or by-products.
EC7: The papers do not contain Isotherms data tables or graphics.

The methodology for selecting and classifying articles was developed using the 4-stage flowchart of the PRISMA Statement (Preferred Reporting Items for Systematic Reviews and Meta-Analysis) (Figure 2).

2.1.4 Information organization and Systematization

After retrieving the 25 studies, specific data fields were extracted separately for each RQ (isotherm type for RQ1, GAB parameters for RQ2, q_{st} values for RQ3, and compositional data for RQ4). The information and data were organized and arranged in matrices and spreadsheets. The matrices included key information such as: (1) Author, (2) Type of product, (3) Study conditions (e.g., temperature), (4) Mathematical isotherm models used (name and equation), (5) Values of the parameters of the models employed, and (6) Reported values of isosteric heat of sorption.

Table 2
Sources and search queries

Source	Search Query	Search fields
Scopus: https://www.scopus.com	"Isosteric heat of sorption" AND "isotherm AND (("food powder" OR "waste" OR)("by-product" NOT "biosorption" NOT "activation"))	Title, Abstract, and Keywords
Sciencedirect: https://www.sciencedirect.com	"Isosteric heat of sorption" AND "isotherm" AND "powder" AND ("waste" AND NOT "biosorption")	Title, Abstract, and Keywords for subscription-access articles. Full-text for Open Access content.
Scielo: https://scielo.org	((isosteric heat of sorption) OR (isotherm)) AND (powder)	Full-text
Redalyc: https://www.redalyc.org	"Isosteric heat of sorption" AND "waste" AND "powders"	Full-text

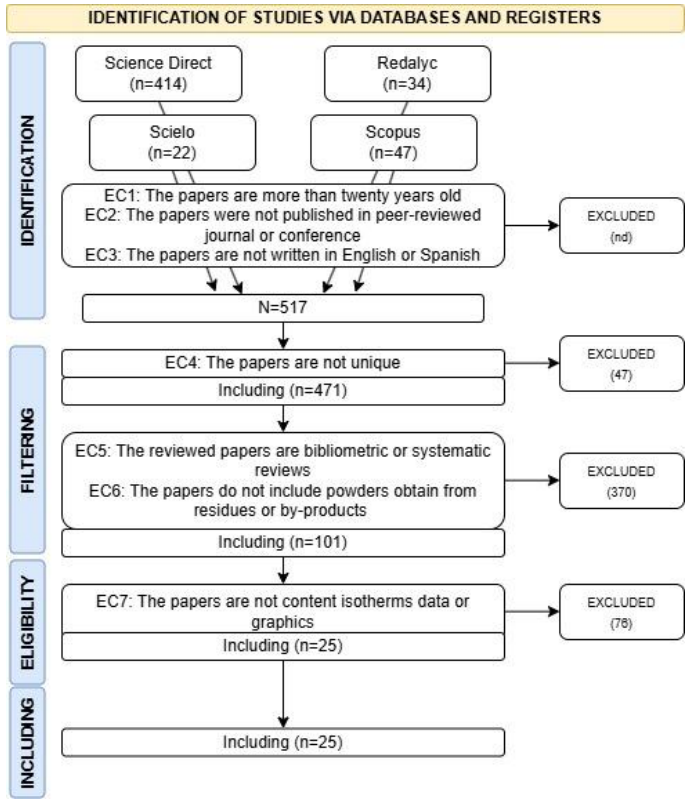

Figure 2. PRISMA Flow Chart.

2.2 Meta-analysis development

2.2.1 Data extraction and mathematical modelling

Values of the isosteric heat of sorption from various powders obtained from agro-industrial by-products were directly collected from studies. However, in cases where the isosteric heat was not directly reported, relevant studies were still included; for these, the necessary data was extracted from sorption isotherms measured at different temperatures, and the corresponding calculations were subsequently performed. To achieve this, the sorption isotherm graphs were extracted as bitmap images and loaded into the xyExtract Graph Digitizer software. The extracted data points from each curve were saved and imported into an Excel spreadsheet for further modeling using the GAB mathematical model (Sarnavi et al., 2023).

The GAB mathematical model (Eq. 1) was used to describe the extracted data from the selected articles. The values of GAB parameters (X_m, C, and K) were identified to minimize the sum of squared errors (SSE, Eq. 2) between the experimental and predicted values. The "Solver" tool in Excel 2016 was used for this purpose, applying the Generalized Reduced Gradient (GRG) algorithm. The goodness of fit of the model was assessed using the coefficient of determination (R^2).

$$X_w = \frac{X_m C K a_w}{(1-a_w)(1-Ka_w+CKa_w)} \quad \text{[Eq. 1]}$$

$$\text{SSE} = \sum_{i=1}^{n}(experimental - calculated)^2 \quad \text{[Eq. 2]}$$

2.2.2 Data calculation

The calculation of the net isosteric heat of sorption (q_{st}) involves the amount of energy required to reduce the moisture content within a food material during the sorption process (Arslan & Toğrul, 2006). This can be determined from the moisture data obtained from sorption isotherms using the Clausius-Clapeyron equation (Eq. 3) (Sarnavi et al., 2023). It is obtained by determining the slope of the plot of ln (a_w) versus 1/T for a specific equilibrium moisture content (X_w) of a given material.

$$\frac{\partial \ln (a_w)}{\partial (1/T)} = -\frac{q_{st}}{R} \quad \text{[Eq. 3]}$$

Where, a_w is the water activity, T is the temperature (K), q_{st} is the net isosteric heat of sorption (kJ/mol), and R is the universal gas constant (8.3144 J/mol K).

2.2.3 Statistical analysis

The results obtained from various studies that focused on calculating the isosteric heat of sorption in by-product powders were systematically compared across different products, and their findings were analyzed and discussed in detail.

Furthermore, a hierarchical cluster analysis was conducted to evaluate the behavior of the parameter X_m (monolayer moisture content in dry

basis) in powdered products, as determined after applying the GAB mathematical model to both adsorption and desorption isotherms. The analysis considered typical adsorption temperatures relevant for powder storage, as well as standard desorption temperatures pertinent to the drying process of powdered products. A dendrogram was constructed using the between-groups linkage method and squared Euclidean distance as the similarity metric, without value transformation. All statistical analyses were performed using SPSS Statistics 23 software (IBM Company, USA).

Additionally, a Principal Component Analysis (PCA) was performed as an exploratory multivariate technique to evaluate the relationships between sorption parameters (X_w, C, K, and temperature) and the compositional classification of powders (fiber, carbohydrate, lipid, and protein). The analysis was conducted separately for adsorption and desorption datasets. Variables were standardized prior to analysis, and group differentiation was visualized using biplots with confidence ellipses. Supplementary projections were also evaluated to assess the representation quality of selected variables.

3. Results and discussion

3.1 Organization and systematization of the information

Table 3 shows the 25 studies included in the development of the systematic review and meta-analysis, which were published between 2007 and 2021. Also presents studies containing adsorption and desorption isotherms, of which 18 studies contain only adsorption isotherms, 3 studies contain only desorption isotherms, and 4 studies include both adsorption and desorption isotherms. Similarly, it was observed that various types of agro-industrial by-products of animal and plant origin were used as raw materials to produce the powders. Additionally, the table specifies the isotherm shape according to the Brunauer classification, distinguishing between type II and type III.

Analysis of selected articles revealed seven categories of predominant compounds present in the different by-product powders: proteins (N° of paper: 1, 6, 7, 11^1, 17, 18), lipids (15, 16), essential oils (2, fiber(2, 3, 4, 8, 11^2, 12^1, 12^2, 13^1, 13^2, 19, 20, 21, 22, 24, 25), anthocyanins (4, 24), starches (5, 10, 14), sugars (9), and chitosan (23). Among these, fiber was the most abundant compound found in by-products studied in the articles included in this research. For more details, see the supplementary material (Tables S1-S5), which provides a structured compilation of information regarding the selected articles that employed the GAB model to describe adsorption and desorption isotherms. For those studies that did not analyze or report the calculation of GAB model parameters and the isosteric heat of sorption, the designation "not reported" was applied, thereby allowing for their subsequent estimation during the meta-analysis phase.

3.2 Powder Sorption Isotherms

Determination of GAB model parameters

Table 4 presents all the studies included incorporating both the reported and calculated (not reported) values of the GAB model parameters. The calculation of the GAB parameters was performed using data extracted from the sorption isotherm curves.

Figures 3 and 4 show examples of the isotherm curve shapes of Type II and Type III, according to Brunauer's classification, for powders derived from Brazilian pine residues (Spada et al., 2013), grape seeds (Bogoeva & Durakova, 2020), mango peels (de Souza et al., 2015), and banana peels (Villa-Vélez et al., 2012) at different temperatures. The curve shapes were obtained by plotting the experimental data (symbols) and the modeled data using the GAB model (dotted lines) of equilibrium moisture content (X_w, g water/g d.m.) versus water activity (a_w). The X_w and a_w data were extracted using the software xyExtract Graph Digitizer.

Figures 5 and 6 illustrate the frequency distribution of evaluation temperatures employed in the selected studies. For adsorption isotherm analyses, the predominant evaluation temperatures for powdered products are within the range of 20 to 30 °C (Figure 5). In contrast, desorption isotherm experiments were most conducted at 40 and 50 °C (Figure 6).

Figures 7 and 8 present the results of the hierarchical cluster analysis. The dendrogram in Figure 7 shows the formation of three groups, indicating that the products within each group do not exhibit significant differences in X_m values. The vertical blue line represents the grouping threshold. Figure 8 displays the formation of four groups, in which the grouping was based on similarities in predominant compound, temperature, or other relevant factors. The vertical blue line indicates the resulting clusters.

3.3 Isosteric heat of sorption in powders

Tables 5 and 6 show the calculated values of isosteric heat of sorption at specific equilibrium moisture contents for each selected article, both for adsorption and desorption. Positive and negative values were observed, reflecting the endothermic and exothermic nature of the sorption process.

Table 3
Articles selected for Systematic review and Meta-analysis

N° of Paper	By-Product	Journal	Sorption Isotherm type and classification	Author	Database source
1	Whey and Spent Coffee ground	Materials Chemistry and Physics	Adsorption isotherm / Type III	(Osorio-Arias et al., 2020)	Scopus/ScienceDirect
2	Lemon peel	LWT - Food Science and Technology	Desorption isotherm / Type III	(García-Pérez et al., 2008)	Scopus/ScienceDirect
3	Orange bagasse	Food Research International	Adsorption isotherm / Type III	(Kaderides & Goula, 2017)	Scopus/ScienceDirect
4	Blueberry pomace	Powder Technology	Adsorption isotherm / Type III	(Tao et al., 2018)	Scopus/ScienceDirect
5	Cassava pomace	Thermochimica Acta	Adsorption isotherm / Type II	(Polachini et al., 2016)	Scopus/ScienceDirect
6	Buffalo whey	Journal of Food Processing and Preservation	Adsorption and Desorption Isotherm / Type II	(Sawhney et al., 2014)	Scopus/ScienceDirect
7	Orange Peel and Whey protein isolate	LWT - Food Science and Technology	Adsorption isotherm / Type II	(Edrisi Sormoli & Langrish, 2016)	Scopus/ScienceDirect
8	Pineapple peel	Journal of Food Process Engineering	Adsorption isotherm / Type III	(Viganõ et al., 2014)	Scopus
9	Yacon bagasse	Food Bioscience	Adsorption isotherm / Type III	(Carvalho Lago & Noreña, 2015)	Scopus/ScienceDirect
10	Pine seed	Journal of Food Engineering	Adsorption isotherm / Type II	(Thys et al., 2010)	Scopus/ScienceDirect
11[1]	Gluten from degermed corn	Food Bioscience	Adsorption and Desorption Isotherm / Type III	(Cristina Duarte Marques et al., 2020)	Scopus/ScienceDirect
11[2]	Fiber from degermed corn				
12[1]	Fermented Cashew shell	Food Bioscience	Desorption isotherm / Type II	(Ribeiro-Filho et al., 2021)	Scopus/ScienceDirect
12[2]	Not Fermented Cashew shell				Scopus/ScienceDirect
13[1]	Fine Wheat bran	Grain & Oil Science and Technology	Adsorption isotherm / Type II	(Li et al., 2021)	Scopus/ScienceDirect
13[2]	Wheat bran 200 µm				Scopus/ScienceDirect
14	Pine seed	Journal of Food Engineering	Adsorption isotherm / Type II	(Spada et al., 2013)	Scopus/ScienceDirect
15	Papaya seed	LWT	Adsorption isotherm / Type II	(Rosa et al., 2021)	Scopus/ScienceDirect
16	Grape seed	Journal of Agriculture and Food Research	Adsorption and Desorption Isotherm / Type II	(Bogoeva & Durakova, 2020)	Scopus/ScienceDirect
17	Whey	Powder Technology	Adsorption isotherm / Type II	(Silva et al., 2015)	Scopus/ScienceDirect
18	Defatted sesame seeds	Journal of Food Engineering	Adsorption isotherm / Type II	(Al-Mahasneh et al., 2007)	Scopus/ScienceDirect
19	Sesame seed hull	Journal of food process engineering	Adsorption isotherm / Type II	(Al-Mahasneh et al., 2010)	Scopus
20	Caltrop skin	Journal of Food Process Engineering	Adsorption isotherm / Type II	(Cheng et al., 2020)	Scopus
21	Banana peel	International Journal of Food Engineering	Desorption isotherm / Type III	(Villa-Vélez et al., 2012)	Scopus
22	Mango peel	Food Science and Technology	Adsorption and Desorption Isotherm / Type III	(de Souza et al., 2015)	Scopus/Scielo
23	Shrimp shell	LWT - Food Science and Technology	Adsorption isotherm / Type II	(Rosa et al., 2010)	Scopus/ScienceDirect
24	Jamun seed	International Journal of Food Studies	Adsorption isotherm / Type III	(Paul & Das, 2019)	Scopus
25	Radish leaf	MATEC Web of Conferences	Adsorption isotherm / Type II	(Ankita & Prasad, 2016)	Scopus

Note: The items listed with superscripts have been separated from the main item based on the by-product used.

Table 4
GAB model parameters reported and calculated (not reported) at different temperatures

N° of Paper	Sorption Isotherm	T ° C	GAB model Parameters			
			X_m	C	K	R^2
1	Adsorption Isotherm	17	0.087	1.177	0.780	-
		26	0.062	2.378	0.825	-
		43	0.044	8.122	0.876	-
2	Desorption Isotherm	20	0.064	4.880	1.000	-
		30	0.069	1.370	1.000	-
		40	0.062	2.300	1.000	-
		50	0.049	4.500	1.000	-
3	Adsorption Isotherm	30	0.0456	5192.480	0.890	0.986
		45	0.0379	5602.390	0.920	0.996
		60	0.0327	5000.000	0.920	0.993
4	Adsorption Isotherm	20	0.045	18.660	1.002	0.999
		35	0.042	17.860	1.024	0.992
		50	0.041	15.320	1.039	0.977
5	Adsorption Isotherm	20	0.056	41.114	0.937	0.999
		30	0.052	64.379	0.938	0.999
		40	0.046	45.529	0.959	0.999
		50	0.040	46.716	0.963	0.999
		55	0.039	47.430	0.961	0.999
		65	0.037	46.086	0.962	0.999
		70	0.035	53.395	0.972	0.998
		75	0.034	45.413	0.965	0.999
		80	0.033	49.519	0.969	0.998
6	Adsorption Isotherm	25	0.051	11.027	1.239	-
		35	0.050	10.213	1.021	-
		45	0.042	14.315	1.403	-
	Desorption Isotherm	25	0.0516	13.210	0.968	-
		35	0.0558	11.509	0.974	-
		45	0.0444	12.008	0.899	-
7	Adsorption Isotherm	30	0.087	9.800	0.990	0.990
		40	0.087	8.830	0.990	0.990
		50	0.087	8.000	0.980	0.990
8	Adsorption Isotherm	40	0.063	1.745	1.011	0.999
		50	0.060	2.272	1.010	0.999
		60	0.086	0.828	0.917	0.999
		70	0.032	3.347	1.016	0.993
9	Adsorption Isotherm	20	0.012	16.829	0.931	0.979
		30	0.010	14.414	0.955	0.982
		40	0.007	18.139	0.993	0.940
		50	0.006	9.075	1.004	0.973
10	Adsorption Isotherm	10	0.100	22.610	0.800	0.990
		20	0.100	28.250	0.670	0.980
		30	0.080	37.870	0.710	0.980
		40	0.070	113.090	0.760	0.950
11[1]	Adsorption Isotherm	20	0.044	1.960	0.780	0.998
		30	0.058	0.080	0.540	0.999
		40	0.036	4.260	0.800	0.998
11[1]	Desorption Isotherm	20	0.051	13.900	0.650	0.993
		30	0.068	3.730	0.530	0.998
		40	0.054	9.600	0.620	0.999
11[2]	Adsorption Isotherm	20	0.037	1.800×10^8	0.140	0.953
		30	0.067	6.510	0.780	0.999
		40	0.065	5.590	0.770	0.998
11[2]	Desorption Isotherm	20	0.039	3.380×10^3	0.110	0.992
		30	0.102	14.200	0.540	0.999
		40	0.087	12.700	0.650	0.999
12[1]	Desorption Isotherm	20	0.360	0.490	0.940	0.969
		30	0.100	0.700	1.120	0.999
		40	0.070	5.670	1.040	0.994
		50	0.090	15.430	0.960	0.973
12[2]	Desorption Isotherm	20	0.240	2.460	1.090	0.975
		30	0.350	0.770	1.020	0.990
		40	0.150	2.270	1.060	0.985
		50	0.120	6.220	1.000	0.991

13[1,a]	Adsorption Isotherm	10	0.091	18.340	0.750	0.997
		20	0.089	12.772	0.744	0.996
		30	0.090	9.007	0.731	0.999
		35	0.091	6.544	0.719	0.999
13[2,a]	Adsorption Isotherm	10	0.092	8.367	0.778	0.997
		20	0.069	9.617	0.837	0.931
		30	0.100	3.454	0.741	0.997
		35	0.124	2.165	0.685	0.996
14 [a]	Adsorption Isotherm	10	0.086	89.268	0.784	0.976
		20	0.071	101.275	0.820	0.955
		30	0.063	55.218	0.838	0.964
15 [a]	Adsorption Isotherm	20	0.175	$1.300x10^6$	0.835	0.983
		30	0.158	$1.930x10^6$	0.850	0.981
		40	0.164	$7.380x10^5$	0.834	0.979
		50	0.165	$2.110x10^5$	0.829	0.971
		60	0.156	$2.380x10^5$	0.845	0.981
		70	0.157	$5.450x10^5$	0.837	0.975
		80	0.151	$1.350x10^6$	0.834	0.968
16 [a]	Adsorption Isotherm	10	0.041	52.430	0.900	0.986
		25	0.053	17.023	0.555	0.990
		40	0.048	17.353	0.623	0.979
	Desorption Isotherm	10	0.061	10.567	0.778	0.959
		25	0.048	22.225	0.688	0.980
		40	0.061	12.805	0.497	0.968
17	Adsorption Isotherm	15	0.138	9.943	0.894	0.997
		25	0.178	8.865	0.821	0.999
		35	0.240	6.114	0.718	0.998
		45	0.320	5.323	0.593	0.996
18 [a]	Adsorption Isotherm	15	0.045	2.542	0.987	0.986
		25	0.053	1.622	0.980	0.983
		35	0.052	2.766	0.989	0.982
		45	0.042	13.480	1.023	0.994
19 [a]	Adsorption Isotherm	15	0.580	0.004	1.145	0.960
		30	0.553	0.031	1.087	0.999
		45	0.536	0.048	1.068	0.999
20	Adsorption Isotherm	20	0.056	3.071	0.862	0.991
		30	0.051	2.383	0.881	0.989
		40	0.041	3.212	0.909	0.968
21 [a]	Desorption Isotherm	20	0.064	1.007	1.095	0.999
		30	0.073	0.994	1.083	0.999
		40	0.068	0.903	1.082	0.999
		50	0.049	1.012	1.092	0.999
		60	0.043	1.059	1.000	0.999
		70	0.039	0.972	1.079	0.999
22 [a]	Adsorption Isotherm	20	0.080	0.737	0.995	0.997
		26	0.090	0.384	0.966	0.995
		33	0.032	2.531	1.060	0.998
		38	0.044	1.336	1.032	0.992
		44	0.032	1.657	1.061	0.997
	Desorption Isotherm	20	0.091	1.026	0.999	0.999
		26	0.086	0.951	0.993	0.999
		33	0.073	0.884	1.012	0.996
		38	0.036	2.519	1.066	0.998
		44	0.031	2.501	1.071	0.997
23	Desorption Isotherm	20	0.200	16.270	0.950	0.996
		30	0.191	12.560	0.930	0.995
		40	0.158	11.710	0.950	0.996
		50	0.133	8.230	0.960	0.996
		60	0.129	2.980	0.950	0.997
24	Adsorption Isotherm	25	0.111	5.277	0.878	0.987
		35	0.096	2.960	0.958	0.984
		45	0.073	3.955	1.045	0.979
25	Adsorption Isotherm	15	0.065	4.912	0.888	0.985
		25	0.071	3.200	0.784	0.995
		35	0.073	2.288	0.730	0.996
		45	0.053	2.451	0.777	0.994

Note: X_m (monolayer moisture content, g water/g d.m.), *C* y *K* (GAB parameters); # [a]: # article with GAB model parameters not reported but calculated in this study; 11[1]: Degermed corn gluten; 11[2]: Degermed corn fiber; 12[1]: Fermented cashew residues; 12[2]: Not fermented cashew residues; 13[1]: Fine wheat bran; 13[2]: Wheat bran 200 µm.

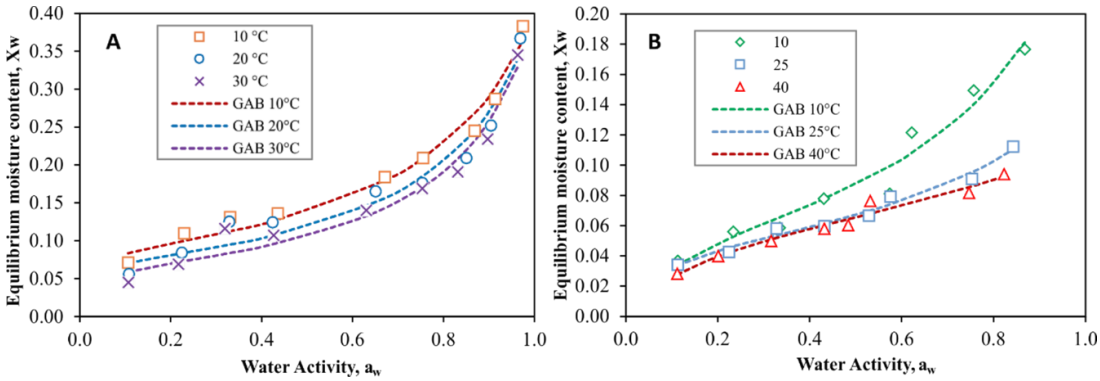

Figure 3. Adsorption isotherm curve shape Type II for Brazilian pine by-product powder (A). Desorption isotherm curve shape type II for Grape seed powder (B).

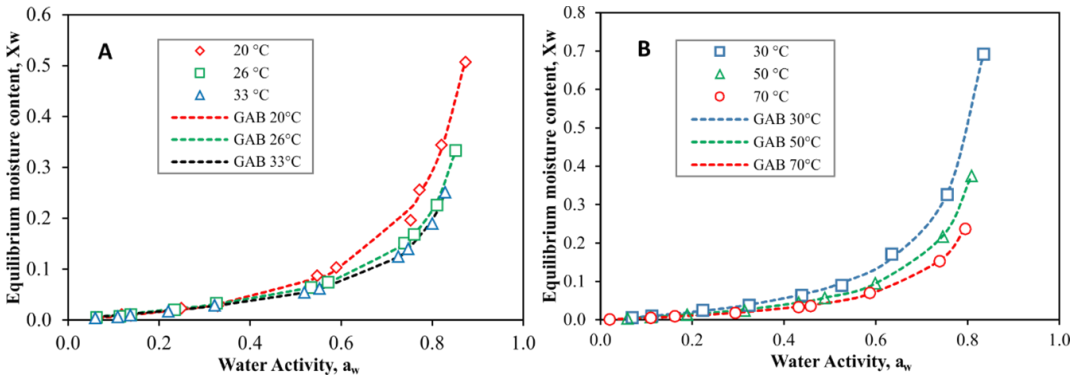

Figure 4. Adsorption isotherm curve shape type III for Mango peel powder (A). Desorption isotherm curve shape type III for Banana peel powder (B).

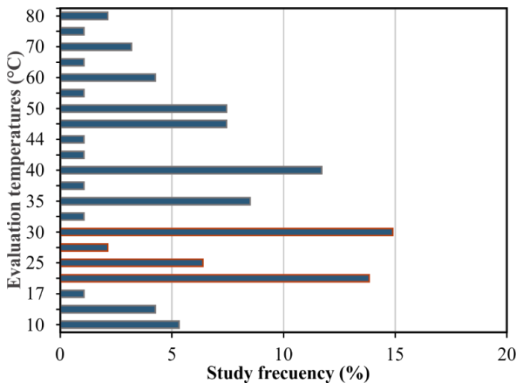

Figure 5. Temperatures of adsorption isotherms and their frequency of use in the selected studies.

Among them, 23 studies analyzed adsorption isotherms, and 10 studies analyzed desorption isotherms. The lowest q_{st} value was observed for the degermed corn gluten powder (Cristina Duarte Marques et al., 2020), while the highest q_{st} value was found in shrimp shell powder (Rosa et al., 2010). Papers numbers 6, 11, 16 and 22 included both adsorption and desorption isotherms. It is evident that q_{st} values are higher in desorption studies than in adsorption at a given X_W, this is the case for mango peel powder, 22[a] (de Souza et al., 2015), where a q_{st} value of 7.22 kJ/mol was observed for desorption and 3.35 kJ/mol for adsorption at X_W = 0.136 g water/g dry matter.

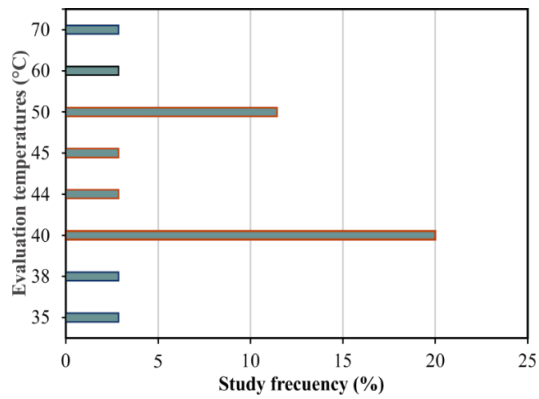

Figure 6. Temperatures of desorption isotherms and their frequency of use in the selected studies.

Based on the results obtained in Tables 5 and 6, two types of energetic behavior of the isosteric heat of sorption (q_{st}) were evident: an endothermic nature with positive values (Figure 9.A) and an exothermic nature with negative values (Figure 9.B).

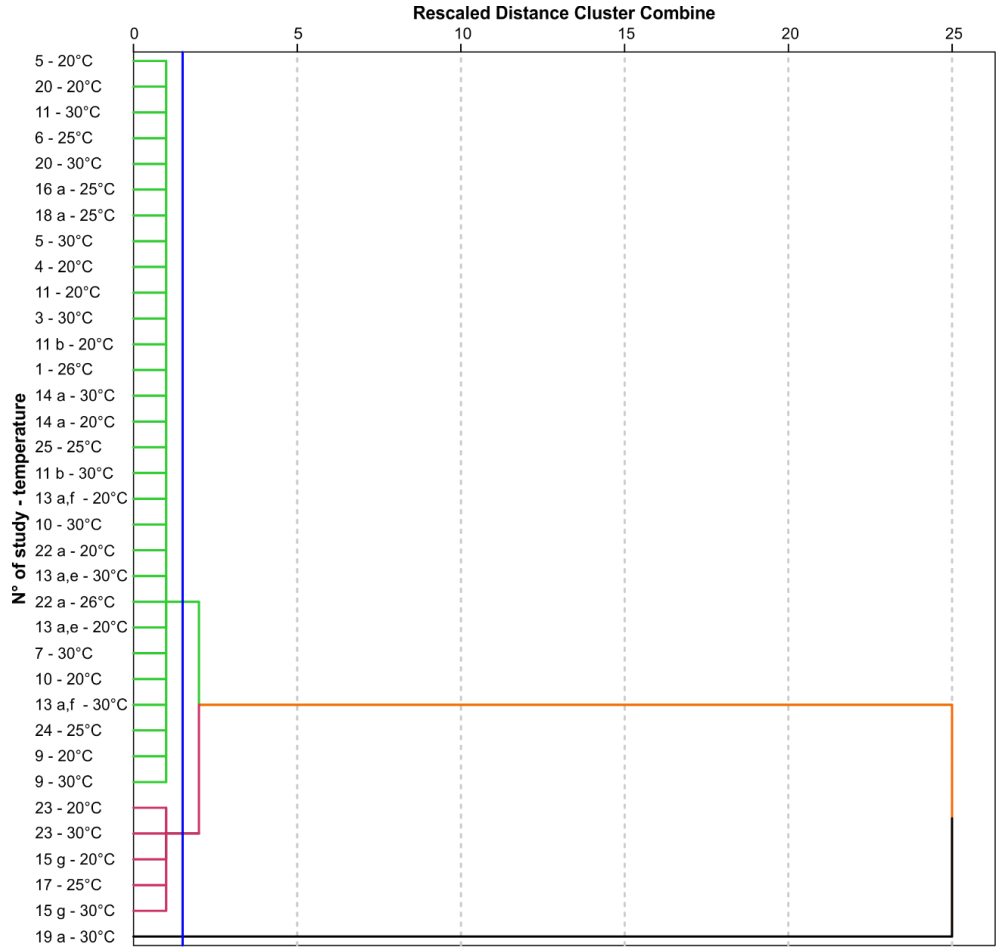

Figure 7. Dendrogram using Average Linkage (Between Groups) of powdered by-products classified by the effect on the X_m parameter, obtained during adsorption at 20–30 °C.

Table 5
Results of adsorption isosteric heat (q_{st} = kJ/mol) obtained at different equilibrium moisture contents

N° of Paper	Equilibrium moisture content (X_W = g water/g dry matter)					
	0.031	0.064	0.111	0.136	0.176	0.22
1	-15.51	-2.19	0.93	1.01	0.74	0.35
3	58.08	13.96	4.11	2.80	1.71	1.06
4	7.58	2.83	0.54	0.16	-0.17	-0.36
5	21.75	13.31	4.49	3.18	2.09	1.46
6	1.74	3.74	-0.29	-1.28	-2.20	-2.77
7	7.63	5.35	2.17	1.43	0.91	0.52
8	11.33	9.34	6.51	5.56	4.51	3.75
9	5.02	0.86	-0.49	-0.80	-1.11	-1.31
10	-20.90	-0.07	15.79	12.01	8.29	6.19
11[1]	-5.05	0.21	0.96	0.89	0.71	0.78
11[2]	521.21	-79.98	-76.69	-74.71	-72.60	-71.15
13[1, a]	27.46	20.61	8.25	5.19	3.13	2.27
13[2, a]	26.78	15.94	5.96	3.72	2.20	1.72
14[a]	32.13	49.63	17.90	10.32	5.46	3.12
15[g]	3.40	3.95	5.89	9.73	4.57	4.16
16[a]	22.58	6.06	7.33	7.75	8.15	8.40
17	2.47	-1.74	-7.78	-10.07	-11.61	-11.04
18[a]	-21.13	-5.89	-1.95	-1.42	-1.06	-0.90
19[a]	-14.34	-9.49	-6.65	-5.77	-4.76	-3.97
20	9.51	6.58	3.43	2.46	1.44	0.74
22[a]	6.63	5.33	3.90	3.35	2.67	2.11
24	21.62	18.70	11.48	8.23	4.52	1.91
25	20.02	13.07	8.25	7.09	6.04	5.41

Note: X_W (Equilibrium moisture, g w/ g dm), q_{st} (sorption isosteric heat, kJ/mol); # [a]: # article with GAB model parameters calculated (not reported); 11[1]: Corn gluten; 11[2]: Corn fiber; 13[1]: Fine wheat bran; 13[2]: Wheat bran 200u; 15 [g]: article with GAB model parameters recalculated.

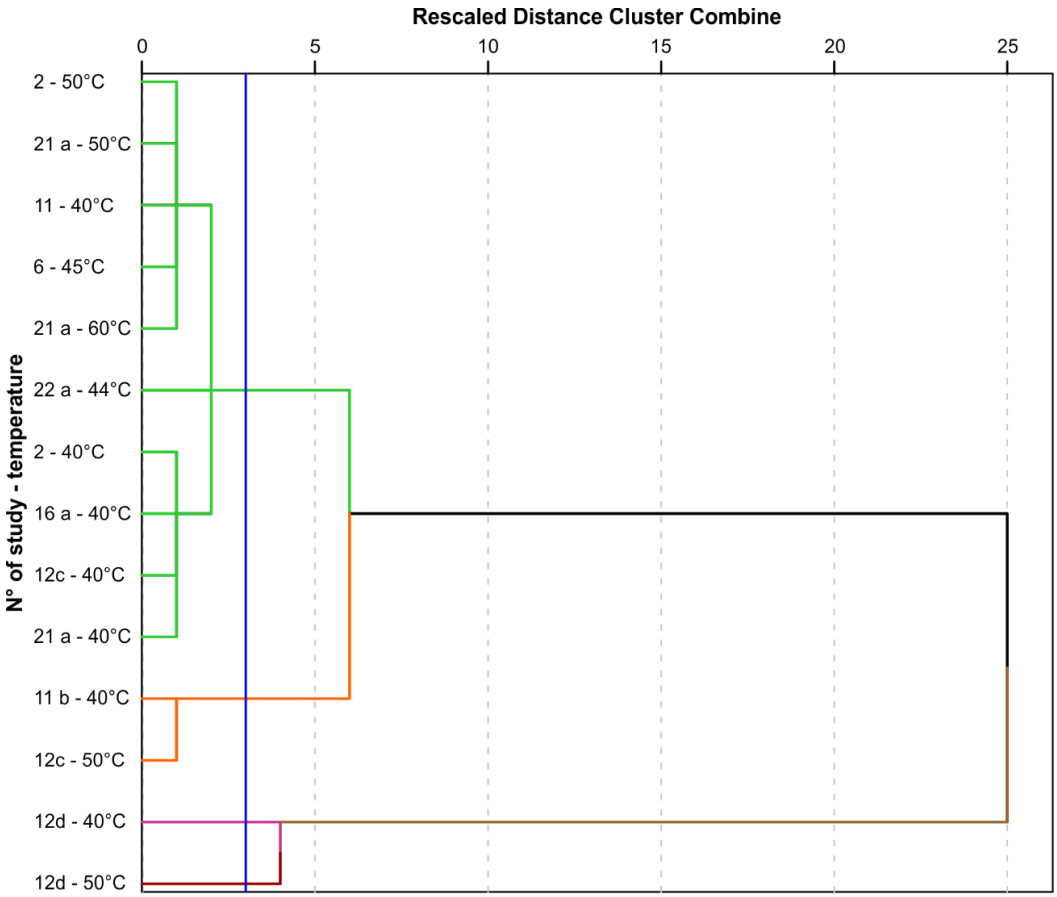

Figure 8. Dendrogram using Average Linkage (Between Groups) of powdered by-products foods classified by the effect on the X_m parameter, obtained during desorption at 40 – 60 °C.

Table 6
Results of desorption isosteric heat (q_{st} = kJ/mol) obtained at different moisture contents

N° of papers	Equilibrium moisture content (X_W)= g water/g dry matter)								
	0.031	0.064	0.111	0.136	0.176	0.22	0.429	0.667	1
2	7.84	6.38	3.93	3.18	2.42	1.91	-	-	-
6	15.73	11.45	6.68	5.73	4.90	2.74	-	-	-
11[1]	9.11	1.77	0.82	0.95	1.13	1.30	-	-	-
11[2]	69.26	-112.04	-94.73	-88.42	-82.57	-79.04	-	-	-
12[1]	-	-	-	0.39	3.94	5.48	6.00	5.06	4.04
12[2]	-	-	-	11.17	12.09	12.03	9.23	7.09	5.53
16[a]	7.35	9.89	10.93	11.00	11.02	11.02	-	-	-
21[a]	6.40	4.63	3.34	2.91	2.41	2.03	-	-	-
22[a]	11.28	10.94	8.37	7.22	5.75	4.55	-	-	-
23	39.48	37.73	33.16	29.70	23.42	17.24	-	-	-

Note: X_W (Equilibrium moisture, g w/g dm), q_{st} (Sorption isosteric heat, kJ/mol); #[a]: # articles with GAB model parameters calculated (not reported); 11[1]: Corn gluten; 11[2]: Corn fiber; 12[1]: Fermented cashew residues; 12[2]: Not fermented cashew residues.

3.4 Multivariate analysis of sorption behavior

To complement the univariate and clustering analyses, and to provide an integrated multivariate perspective on the relationships between sorption parameters and compositional characteristics of powdered by-products, a Principal Component Analysis (PCA) was performed for both adsorption and desorption datasets.

The suitability of the dataset for PCA was evaluated using the Kaiser–Meyer–Olkin (KMO) test and Bartlett's test of sphericity. For adsorption, the KMO value was 0.47, indicating low sampling adequacy, while Bartlett's test was significant (χ^2 = 27.99, p < 0.001), confirming the presence of correlations among variables. For desorption, the KMO value increased to 0.52, indicating acceptable sampling adequacy, with Bartlett's test remaining highly significant (χ^2 = 40.84, p < 0.001). Despite the relatively low KMO value for adsorption, this limitation is expected given the inherent heterogeneity of datasets

derived from meta-analyses, where variables originate from different experimental conditions and materials. Therefore, PCA remains suitable as an exploratory tool for identifying general patterns. The first two principal components explained approximately 67% – 70% of the total variance in both adsorption and desorption datasets, indicating that the biplot representation captured most of the variability and provided a reliable visualization of the relationships among variables.

In adsorption (Figure 10), a clear separation of compositional groups was observed along the first principal component (PC1). Carbohydrate- and lipid-rich powders were primarily associated with positive PC1 values and showed a strong relationship with the parameter C (logC), reflecting stronger water–solid interaction energies. In contrast, fiber-rich powders were distributed towards negative PC1 values and showed a closer association with X_m, suggesting a dominant role of structural water binding and multilayer formation.

Protein-based powders were more centrally distributed but exhibited partial alignment with temperature (T), indicating a moderate influence of thermal conditions on their sorption behavior.

In desorption (Figure 11), a similar structure was observed, although with a more pronounced separation driven by temperature and the parameter K, suggesting higher energy requirements during water removal. Fiber-rich powders showed wider dispersion, reflecting greater variability in their sorption behavior under desorption conditions.

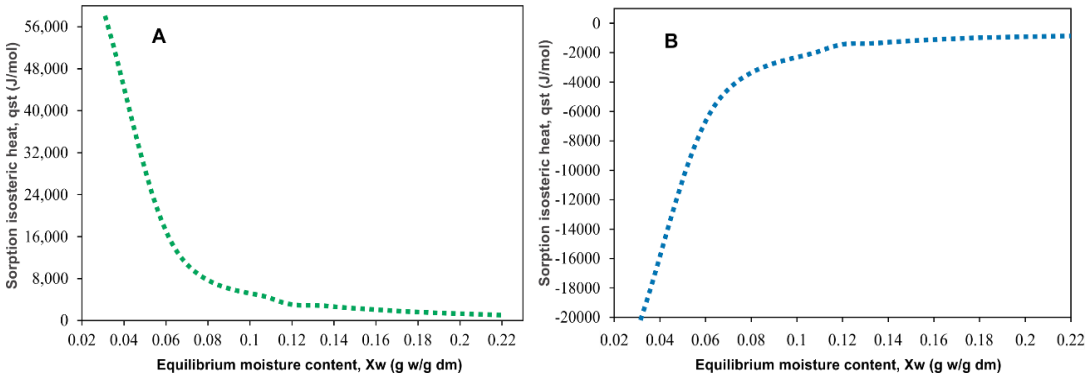

Figure 9. A: Endothermic nature of q_{st} for powder made from orange waste residue (Kaderides & Goula, 2017). B: Exothermic nature of q_{st} for powder made from whey and coffee ground waste (Osorio-Arias et al., 2020).

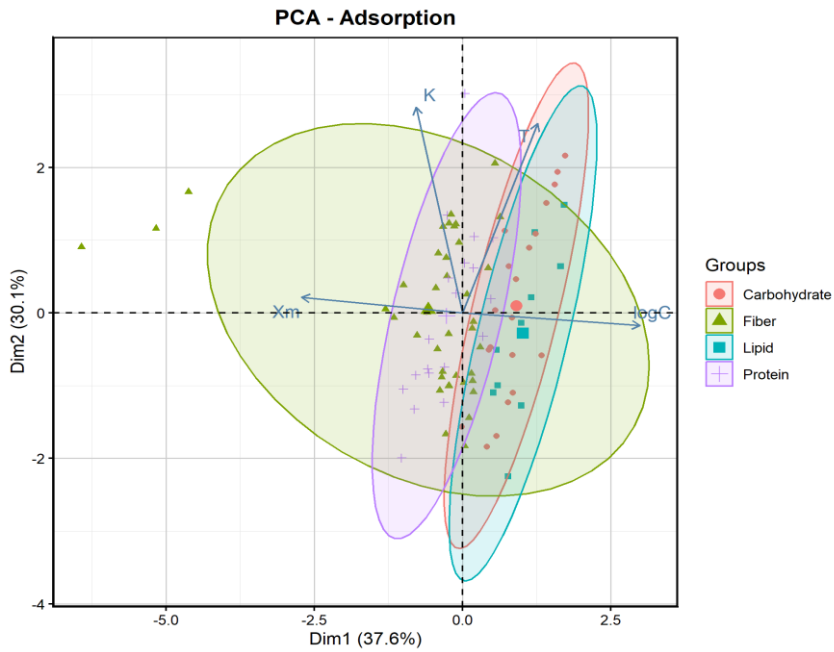

Figure 10. Principal Component Analysis (PCA) biplot for adsorption data showing the relationships between GAB parameters (X_m, LogC, K), temperature (T), and compositional groups (carbohydrate, fiber, lipid, and protein) in powdered agro-industrial by-products. Ellipses represent group dispersion.

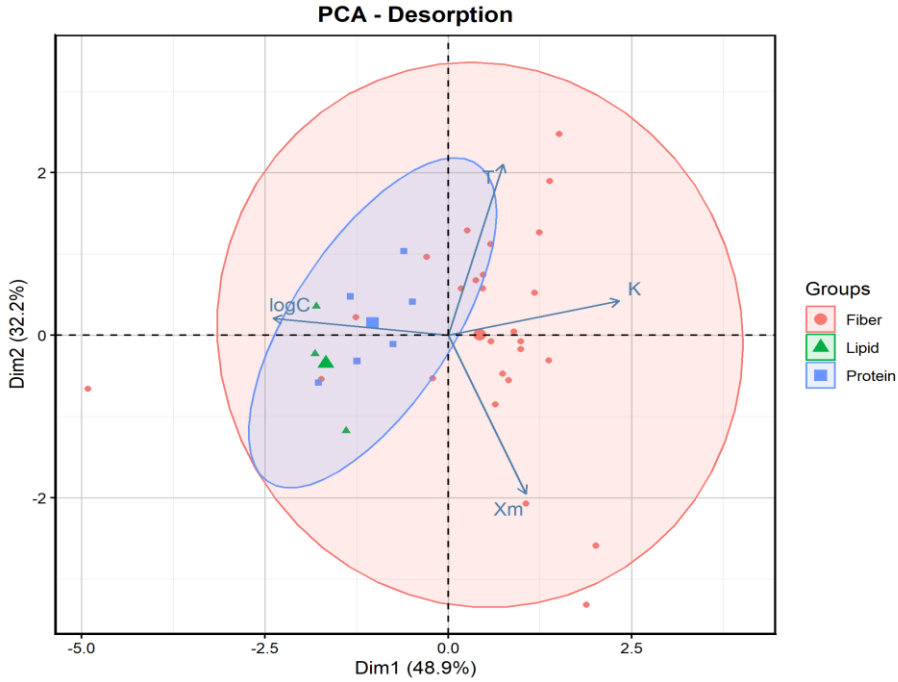

Figure 11. Principal Component Analysis (PCA) biplot for desorption data showing the relationships between GAB parameters (X_m, LogC, K), temperature (T), and compositional groups (fiber, lipid, and protein) in powdered agro-industrial by-products. Ellipses represent group dispersion.

Overall, the PCA results indicate that sorption behavior in powdered by-products is primarily structured by compositional factors and their interaction with GAB parameters. Carbohydrate and lipid fractions are more closely associated with energetic interactions (parameter C), while fiber-rich matrices are more related to structural water retention (X_m). These multivariate patterns are consistent with the clustering results, where groups were primarily structured according to compositional similarities and X_m values, reinforcing the role of composition and structural factors as key drivers of sorption behavior.

The isosteric heat of sorption (q_{st}) was initially included in the PCA as a supplementary variable to evaluate its relationship with the main sorption parameters. However, q_{st} showed very low representation in the principal component space ($\cos^2 < 0.03$ for PC1–PC2), indicating a negligible contribution to the explained variance.

Additional projections (PC2–PC3) were evaluated, but no improvement in its representation was observed. This suggests that sorption energetics are not strongly aligned with the structural variability captured by the GAB parameters and temperature. Therefore, q_{st} was excluded from the graphical representation to preserve clarity and interpretability of the biplots. Nevertheless, its thermodynamic behavior and relevance are discussed in detail in Section 4.3.

4 Analysis of results and answers to research questions

4.1 Type of sorption isotherms and their relation to powder composition (Related to RQ1)

The analysis of sorption isotherms in powdered foods at different temperatures is essential to predict shelf-life stability and determine the final moisture content during the drying process (Edrisi Sormoli & Langrish, 2016). It also provides important information for the design of drying equipment, packaging type, study of water–food component interactions and helps to estimate the drying process limit (Corrêa et al., 2017; Simal et al., 2007). Sorption isotherms are represented through the variation of equilibrium moisture content versus water activity of a given food material.

From the information search, two types of isotherms were identified according to Brunauer's classification, in addition to the predominant compound based on the analyzed study. The isotherm type describes the shape of the sorption isotherm experimentally plotted using the a_w and X_W data (Figures 4, and 5). According to recent studies, powdered foods generally exhibit type II or III isotherms, depending on their composition and processing conditions (Acurio et al., 2024; Cheng et al., 2023; Siqueira-de-Lima et al., 2024). Table 4 details the major compound, type of residue, type of sorption isotherm studied, and article number based on Brunauer's type II and III isotherm classification.

Muzaffar & Kumar (2016) state that the shape of the curve results from the moisture sorption processes within the porous structure of foods and depends on factors such as the chemical composition of the food material.

Type II isotherms (Figures 4A and 4B) show a sigmoidal-shaped curve consisting of three regions: the first corresponds to the strong binding of monolayer moisture; the second, linear in form, corresponds to multilayer water; and the third region to the availability of free water (Brunauer et al., 1940). This type is characteristic of porous materials with high adsorption energies (Silva et al., 2015) and particularly typical of powdered foods derived from residues of tubers, fruits, cereals, and other grains (Prasantha, 2018), which are mostly composed of proteins, starch, and biopolymers like maltodextrins (Sawhney et al., 2014). On the other hand, type III isotherms (Figures 5A and 5B) are characteristic of products containing small amounts of water with low water activity and large amounts of water with high relative humidity. This behavior is typical of materials with relatively high fiber, protein, and sugar content (Kaderides & Goula, 2017). This statement was confirmed by Carvalho Lago & Noreña (2015), who found 67% carbohydrates and sugar compounds in powdered yacon bagasse. This type of isotherm occurs when the monolayer binding energy is lower than the water molecule binding energy due to the high carbohydrate and sugar content.

4.2 GAB Parameters and X_m values for stability of by-product powders (Related to RQ2)

To understand the behavior of sorption isotherms in food powders produced from agro-industrial by-products, the GAB mathematical model (Equation 1) was used. Table 3 shows the GAB model parameters of the different analyzed studies, with R^2 values higher than 0.90. The authors in the included articles demonstrate that the GAB model (Equation 1) accurately represents sorption isotherms in foods rich in fiber, starch, proteins, sugars, etc.

The GAB model (Equation 1) provides valuable information to understand the behavior of water within a food matrix, through the analysis of its parameters such as the monolayer moisture content (X_m) and the constants *C* and *K*. In some included studies where GAB parameters are not reported, they were calculated. For this, a_w and X_W data at a certain temperature were extracted using the XYExtract Graph Digitizer software, and then the GAB model parameters were calculated using the sum of squared errors (SSE) with the Excel 2016 "Solver" tool. This method was applied to powders produced from agro-industrial residues, including wheat bran, pine seed, grape seed, sesame peel, mango peel, and banana peel residues (Al-Mahasneh et al., 2007, 2010; Bogoeva & Durakova, 2020; de Souza et al., 2015; Li et al., 2021; Spada et al., 2013; Villa-Vélez et al., 2012). Additionally, the GAB parameters for the papaya seed powder study (Rosa et al., 2021) were recalculated due to the presence of high monolayer values (X_m).

When experimentally analyzing the sorption isotherm curves at the corresponding study temperature, it was shown that temperature has a significant effect on the sorption isotherm, since foods are exposed to different temperatures during storage and processing, and their water activity (a_w) changes with equilibrium moisture content (X_W) at the same temperature. At constant temperature, some studies showed a progressive increase in X_W with increasing a_w. However, Kaderides & Goula (2017) reported a slight increase in X_W in the initial stage of the isotherm curve up to a water activity of 0.55 in orange bagasse powder. Likewise, some researchers found significant increases in X_W with temperature increases at a_w values above 0.55, due to rapid migration of water molecules into the food matrix, leading to sugar dissolution, as sugar-rich foods can become more hygroscopic.

The study of monolayer moisture content (X_m) represents the binding of water molecules that form a monolayer at sorption sites. In other words, it indicates the safe moisture level for powdered food during storage, meaning that values at or below this level lead to minimal quality deterioration rates in such foods at a given temperature (Osorio-Arias et al., 2020). This value is of great importance for describing the physicochemical stability of dried foods with respect to enzymatic activity, enzymatic browning, lipid oxidation, and the preservation of organoleptic components (Arslan-Tontul et al., 2024). The formation of multilayers causes food deterioration due to the generation of several layers, as the adsorption sites are occupied by weakly bound water molecules (Carvalho Lago & Noreña, 2015).

Table 3 shows that at constant water activity, a decrease in X_m was observed with increasing temperature (Tao et al., 2018), with X_m values ranging from 0.6 to 0.006 g water/g d.m. at a study temperature range of 20 to 80 °C. In the "not reported" studies, a decrease in X_m with increasing temperature was evident in pine seed powder, sesame peel powder, and mango peel powder (Al-Mahasneh et al., 2010; de Souza et al., 2015; Spada et al., 2013), with values ranging from 0.03 to 0.5 g water/g d.m. at a study temperature of 10 to 50 °C respectively. This

behavior is attributed to the reduction of sorption sites caused by physical and chemical changes due to increased temperature. The reduction of sorption sites is due to the activation of water molecules to maximum energy levels caused by increased temperature, making the water molecules unstable and detach from the sorption sites in the food (Fan et al., 2015). The same behavior can be attributed to foods rich in sugar and antioxidants (Edrisi Sormoli & Langrish, 2016). This behavior is characteristic of adsorption phenomena. However, several researchers found high X_m values; according to Tao et al. (2018) this value may be due to the bonding of water molecules with a greater number of polar groups and sugars. This assertion is supported in food powders with high fiber and protein content with X_m values from 0.53 to 0.10 g water/g d.m. at a temperature range of 15 to 45 °C, for powders of cashew peel, whey, sesame seed hulls, and shrimp shells (Al-Mahasneh et al., 2010; Ribeiro-Filho et al., 2021; Rosa et al., 2010; Silva et al., 2015). In studies analyzing adsorption and desorption isotherms, X_m values were generally higher in desorption studies, with values of 0.516 vs. 0.512 g water/g d.m., 0.051 vs. 0.044 g water/g d.m., 0.06 vs. 0.04 g water/g d.m., and 0.091 vs. 0.081 g water/g d.m. for buffalo whey powder, defatted corn fiber and gluten powder, grape seed powder, and mango peel powder, respectively (Bogoeva & Durakova, 2020; Cristina Duarte Marques et al., 2020; de Souza et al., 2015; Sawhney et al., 2014).

Regarding the GAB parameters *C* and *K*, they are related to the interaction energy between water molecules and compounds in the product (Sahu et al., 2021). The "*C*" parameter indicates the strength that holds the water molecules to the primary binding sites on the food surface. High *C* values indicate greater affinity between the water molecules and the binding sites on the adsorbent surface (Aouaini et al., 2016). The "*K*" parameter is a measure of the interactions between bulk liquid water molecules and those absorbed in the multilayer; when *K* approaches one, the molecules further from the monolayer resemble pure water (a_w = 0.9). When K = 1, the GAB equation reduces to the BET equation. Likewise, when *K* is greater than 1, the sorption isotherm becomes infinite at a_w < 1 (Arthur et al., 2018).

The frequency of temperature levels used in the selected studies is shown in Figures 5 and 6. For adsorption isotherm studies, monolayer values (X_m) at typical storage temperatures for powdered products (20 to 30 °C) are important, coinciding with the most studied range (Figure 5). For desorption isotherm studies, X_m values at typical drying temperatures for such products (40 to 60 °C) are important; however, most studies were conducted at 40 and 50 °C (Figure 6).

Hierarchical cluster analysis was performed using SPSS Statistics 23 software. The graph in Figure 7 shows the formation of three groups, demonstrating that the products within each group show no significant differences regarding their X_m values. The first group includes most products with X_m values below 0.17 d.m. The second group consists of powdered products with X_m values ranging from 0.17 to 0.2. Finally, the powder obtained from sesame seed hulls differs from all the others due to presenting the highest value. Figure 8 shows the formation of four groups, based on the coincidence within groups regarding the predominant compound and the temperature. The first group includes most of the powdered products rich in protein and fiber, with X_m values ranging from 0.042 to 0.054 (g water/ g d.m.). The second group consists of products rich in fiber and oils, with X_m values ranging from 0.06 to 0.07 (g water/ g d.m.). The third group comprises products that are predominantly rich in fiber, with X_m values ranging from 0.086 to 0.09 (g water/ g d.m.). Finally, the fourth group includes the X_m values of the powdered product derived from cashew by-products, which exhibit X_m values greater than 0.12 (g water/ g d.m.). In addition, the multivariate analysis (PCA) confirmed that the monolayer moisture content (X_m) is strongly associated with fiber-rich matrices, reflecting their structural role in water retention. This supports the interpretation of X_m as a parameter linked to the physical binding and multilayer formation of water molecules within the food matrix.

4.3 Typical range and thermal nature of isosteric heat of sorption in by-product powders (Related to RQ3)

The isosteric heat of sorption (q_{st}) estimates the amount of energy required to break the forces that bind water molecules to the surface of a food matrix (Edrisi Sormoli & Langrish, 2016; Prasantha, 2018). This property also provides valuable information about the state of adsorbed water, serving as an indicator of stability during storage (Tadapaneni et al., 2017; Viganõ et al., 2014).

In all the included studies, the q_{st} value was calculated. For this purpose, water activity (a_w) at two or more temperatures was needed, and q_{st} was determined by plotting ln(a_w) versus 1/T (absolute temperature) at a given moisture content. The q_{st} was obtained from the slope of the graph (Sahu et al., 2021). For the meta-analysis, equilibrium moisture content (X_W) values of 0.031, 0.064, 0.111,

0.136, 0.176, and 0.220 g water/g dry matter (d.b.) were used for both adsorption and desorption processes.

The q_{st} results revealed two types of energetic conditions. An endothermic character was observed in most studies, attributed to the positive nature of the data due to the energy released until a stable product is reached. This behavior was reported by Kaderides & Goula (2017) for orange waste powders, with q_{st} values of 58.0 kJ/mol and 13.9 kJ/mol for X_W values of 0.031 and 0.064 g water/g d.b., respectively (Table 4 and 5). Conversely, negative q_{st} values with an exothermic character were also observed when energy is absorbed to break the forces binding water molecules to the food surface. This behavior was noted by (Osorio-Arias et al., 2020) for whey residue and spent ground coffee powders, with q_{st} values of -15.5 kJ/mol and -2.18 kJ/mol for X_W values of 0.031 and 0.064 g water/g d.b., respectively. Similar exothermic behavior was also observed in studies by Al-Mahasneh et al. (2007), Cristina Duarte Marques et al. (2020), Silva et al. (2015), and Al-Mahasneh et al. (2010) for defatted sesame seed powder, degermed corn fiber powder, whey powder, and sesame seed shell powder.

A comparison was made between the reported and recalculated q_{st} values (Tables 4 and 5). The results showed good agreement. For example, for orange bagasse powder (Kaderides & Goula, 2017), a reported q_{st} value greater than 42 kJ/mol was observed when X_W was below 0.08 g water/g d.b., while the recalculated q_{st} was 58.0 kJ/mol at X_W = 0.031 g water/g d.m.; for orange peel powder (Edrisi Sormoli & Langrish, 2016), a reported q_{st} of 7.9 kJ/mol and a recalculated value of 7.6 kJ/mol at X_W = 0.031 g water/g d.m.; and for pineapple peel powder (Viganõ et al., 2014), a reported $\boldsymbol{q_{st}}$ of 11.4 kJ/mol and recalculated value of 11.3 kJ/mol at X_W = 0.031 g water/g d.m.

However, the PCA results indicated that the isosteric heat of sorption (q_{st}) is not strongly aligned with the main structural variables (X_m, C, and K), suggesting that sorption energetics behave independently from the structural parameters described by the GAB model. This reinforces the idea that q_{st} reflects energetic interactions at a molecular level rather than bulk structural properties.

4.4 Compositional drivers of q_{st} variability (Related to RQ4)

The variability of isosteric heat of sorption (q_{st}) can be better understood by integrating the multivariate and clustering analyses. PCA confirmed that compositional fractions influence sorption behavior through distinct mechanisms, where structural parameters and energetic interactions are governed by different components of the food matrix.

In adsorption studies, q_{st} values greater than 9.7 kJ/mol at X_W = 0.136 g water/g d.m. were observed for pine seed powder (Spada et al., 2013; Thys et al., 2010), likely due to its high starch content and porous structure, which requires more energy to remove water molecules from sorption sites (Silva et al., 2015). Papaya seed powder (Rosa et al., 2021), due to its lipid content, showed a reduction in polar sites. Meanwhile, for desorption studies, q_{st} values greater than 11.0 kJ/mol at X_W = 0.136 g water/g d.m. were reported for grape seed powder (Bogoeva & Durakova, 2020), unfermented cashew peel powder (Ribeiro-Filho et al., 2021), and shrimp shell powder, with a value of 29.7 kJ/mol at X_W = 0.136 g water/g d.m. (Rosa et al., 2010), due to its high chitosan content.

For desorption studies, q_{st} values were higher than those from adsorption at X_W values of 0.136 and 0.176 g water/g d.m. (Tables 4 and 5). This may be attributed to the greater energy requirements during desorption and possible structural changes during the sorption process (Edrisi Sormoli & Langrish, 2016), as shown for buffalo whey powder, gluten and degermed corn fiber powder, grape seed powder, and mango peel powder (Bogoeva & Durakova, 2020; Cristina Duarte Marques et al., 2020; de Souza et al., 2015; Sawhney et al., 2014).

On the other hand, according to Carvalho Lago & Noreña (2015), at the beginning of the sorption process, there is a strong dependence between the isosteric heat of sorption (q_{st}) and the equilibrium moisture content (X_W). High q_{st} values were found at low X_W, attributed to the presence of highly active polar sites on the food surface, leading to greater water-solid interaction energy (Edrisi Sormoli & Langrish, 2016). These highly active sorption sites cause water molecules to bind strongly, thus requiring more energy to remove the water from the interaction bonds. Likewise, other q_{st} values were below 8 kJ/mol at X_W = 0.136 g water/g d.m. It is also evident that q_{st} tends to become constant beyond X_W = 0.136 g water/g d.m., as water molecules behave as free water in the product, as observed in grape seed powder (Bogoeva & Durakova, 2020). However, at X_W = 0.136 g water/g d.m., negative values were found: -74.7 kJ/mol for degermed corn fiber powder (Cristina Duarte Marques et al., 2020), -10.1 kJ/mol for whey powder (Silva et al., 2015) in adsorption studies due to their high protein content, and -88.4 kJ/mol for degermed corn fiber powder (Cristina Duarte Marques et al., 2020) in desorption studies.

To further strengthen the interpretation of compositional effects, a multivariate analysis (PCA) was incorporated to evaluate the relationships between sorption parameters and the main components of powdered by-products. The PCA results revealed a clear structural organization of the variables, where carbohydrate- and lipid-rich powders were primarily associated with the parameter C (logC), reflecting stronger energetic interactions between water molecules and sorption sites (Edrisi Sormoli & Langrish, 2016; Sahu et al., 2021). In contrast, fiber-rich matrices showed a stronger association with the monolayer moisture content (X_m), indicating their dominant role in structural water retention and multilayer formation (Carvalho Lago & Noreña, 2015). Protein-based powders exhibited intermediate behavior, showing partial alignment with temperature, which suggests a combined influence of both structural and thermal factors on their sorption properties.

Interestingly, despite its thermodynamic relevance, the isosteric heat of sorption (q_{st}) did not show a significant contribution in the principal component space, indicating that its variability is not directly aligned with the structural parameters described by the GAB model. This suggests that q_{st} reflects localized molecular interactions rather than global structural properties, as previously reported in sorption thermodynamics studies (Arslan & Toğrul, 2006).

These findings indicate that different compositional fractions control sorption behavior through distinct mechanisms: carbohydrates and lipids mainly influence the energetic interactions (parameter C), while fiber contributes to the structural organization and water-holding capacity (X_m). Therefore, sorption behavior in powdered agro-industrial by-products can be interpreted as the result of a dual mechanism: (i) structural effects associated with matrix composition, captured by X_m and clustering patterns, and (ii) energetic interactions at the molecular level reflected by q_{st}, which remain partially independent from structural variability. This distinction provides a more robust framework for optimizing drying processes and storage conditions.

4. Conclusions

This study conducted a systematic review and meta-analysis on the isosteric heat of sorption in food powders derived from agro-industrial residues. From a total of 518 identified studies, 25 met the inclusion criteria and were analyzed. The results showed that these powders predominantly exhibit Type II and Type III sorption isotherms, which are strongly influenced by their chemical composition. Type II isotherms were associated with materials rich in starch, proteins, and structural biopolymers, while Type III behavior was mainly linked to sugar- and fiber-rich matrices.

The GAB model proved to be the most suitable for describing sorption isotherms, with R^2 values exceeding 0.90 across studies. The monolayer moisture content (X_m), which represents the optimal moisture level for product stability, generally decreased with increasing temperature. Higher X_m values were observed in desorption compared to adsorption, indicating greater water retention during drying processes.

The hierarchical cluster analysis allowed the classification of powdered by-products based on X_m values and compositional similarities, revealing distinct groups associated with fiber, protein, and lipid content, as well as processing temperature. These clustering patterns, together with PCA results, highlight the key role of composition and thermal conditions in defining both structural water retention and sorption energetics.

The isosteric heat of sorption (q_{st}) showed a wide range of values, including both endothermic and exothermic behaviors, depending on moisture content and material composition. At low equilibrium moisture contents, higher q_{st} values were observed due to the presence of highly active polar sites, while at higher moisture levels, q_{st} tended to stabilize as water molecules behaved more like free water.

The incorporation of multivariate analysis (PCA) provided a deeper understanding of the relationships between compositional factors and sorption behavior. The results revealed that structural parameters such as X_m are mainly associated with fiber-rich matrices, while energetic interactions represented by the GAB parameter C are more closely related to carbohydrate and lipid fractions. In contrast, the isosteric heat of sorption (q_{st}) showed a weak association with the principal components, indicating that sorption energetics are not directly aligned with the structural variability described by GAB parameters but rather reflect localized molecular interactions.

Overall, the combined use of hierarchical clustering and PCA demonstrates that sorption behavior in powdered agro-industrial by-products is governed by a dual mechanism involving (i) structural factors associated with matrix composition and water retention (X_m), and (ii) energetic interactions at the molecular level reflected by q_{st}. This integrated perspective is essential for improving the design of drying processes and optimizing storage stability.

Future research should focus on the standardization of methodologies for determining q_{st}, particu-

larly regarding equilibrium moisture ranges and experimental conditions. In addition, the integration of multivariate approaches and predictive modeling is recommended to better link structural parameters (e.g., GAB model) with energetic properties. Further experimental studies under controlled and comparable conditions are also required to reduce methodological variability and to support the optimization of drying processes and storage stability.

Authors contribution

M. Chamache: Methodology, Data curation, Investigation, Writing – original draft, Visualization. **M. L. Rojas:** Conceptualization, Methodology, Formal Analysis, Investigation, Writing – review & editing, Visualization. **G. Linares:** Conceptualization, Methodology, Investigation, Writing – review & editing, Supervision.

Conflict of Interest Statement

The authors declare that they have no conflict of interest regarding the publication of this paper.

ORCID

M. Chamache https://orcid.org/0009-0008-3510-202X
M. Lindsay Rojas https://orcid.org/0000-0001-5750-8399
G. Linares https://orcid.org/0000-0003-3889-4831

References

Acurio, L., Salazar, D., García, M. E., García-Segovia, P., Martínez-Monzó, J., & Igual, M. (2024). Characterization, mathematical modeling of moisture sorption isotherms and bioactive compounds of Andean root flours. *Current Research in Food Science*, *8*. https://doi.org/10.1016/j.crfs.2024.100752

Ahmad, T., Esposito, F., & Cirillo, T. (2024). Valorization of agro-food by-products: Advancing sustainability and sustainable development goals 2030 through functional compounds recovery. In *Food Bioscience* (Vol. 62). Elsevier Ltd. https://doi.org/10.1016/j.fbio.2024.105194

Al-Mahasneh, M. A., Rababah, T. M., Al-U'Datt, M. H., & Yang, W. (2010). Moisture adsorption thermodynamics of fractionated sesame hulls (sesamum indicum l.). *Journal of Food Process Engineering*, *33*(5), 802–819. https://doi.org/10.1111/j.1745-4530.2008.00306.x

Al-Mahasneh, M. A., Rababah, T. M., & Yang, W. (2007). Moisture sorption thermodynamics of defatted sesame meal (DSM). *Journal of Food Engineering*, *81*(4), 735–740. https://doi.org/10.1016/j.jfoodeng.2007.01.010

Ankita, & Prasad, K. (2016). Adsorption Studies of Radish Leaf Powder. *MATEC Web of Conferences*, *57*. https://doi.org/10.1051/matecconf/20165704002

Aouaini, F., Knani, S., Ben Yahia, M., Bahloul, N., Ben Lamine, A., & Kechaou, N. (2016). New insights on energetic analysis of water adsorption isotherms of the Pelargonium graveolens: Modeling, interpretations and pore sizes distribution based on statistical physics approach. *RSC Advances*, *6*(63), 58796–58804. https://doi.org/10.1039/c6ra06559g

Arslan, N., & Toğrul, H. (2006). The fitting of various models to water sorption isotherms of tea stored in a chamber under controlled temperature and humidity. *Journal of Stored Products Research*, *42*(2), 112–135. https://doi.org/10.1016/j.jspr.2005.01.001

Arslan-Tontul, S., Gunisik, A., & Tontul, I. (2024). Moisture sorption isotherm and thermodynamic analysis of egg powders dried by foam-mat-assisted refractance window drying. *Journal of the Science of Food and Agriculture*, *104*(14), 8646–8654. https://doi.org/10.1002/jsfa.13692

Arthur, E., Tuller, M., Moldrup, P., Greve, M. H., Knadel, M., & de Jonge, L. W. (2018). Applicability of the Guggenheim–Anderson–Boer water vapour sorption model for estimation of soil specific surface area. *European Journal of Soil Science*, *69*(2), 245–255. https://doi.org/10.1111/ejss.12524

Balakrishnan, S., Chandrasekaran, I. R., Jegadeesan, R., Ramachandran, K., Govindasamy, A. K., & Kandasamy, G. (2025). Eco-innovation in action: valorizing vegetable waste into high-value ingredients for sustainable applications. In *Frontiers in Sustainable Food Systems* (Vol. 9). Frontiers Media SA. https://doi.org/10.3389/fsufs.2025.1507120

Bogoeva, A. L., & Durakova, A. G. (2020). Sorption characteristics of full-fatted grape seeds flour of Bulgarian origin. *Journal of Agriculture and Food Research*, *2*. https://doi.org/10.1016/j.jafr.2020.100026

Boudalia, S., Symeon, G. K., Dotas, V., Gueboudji, Z., Kouadri, I., Sehili, B., Terfa, M. T., Smeti, S., Gueroui, Y., & Bousbia, A. (2026). The Valorization of Agrifood Byproducts and Waste to Advance the Sustainable Development Goals: Current State and New Perspectives. *Sustainability*, *18*(5), 2165. https://doi.org/10.3390/su18052165

Brunauer, S., Deming, L. S., Deming, W. E., & Teller, E. (1940). *On a Theory of the van der Waals Adsorption of Gases*. https://doi.org/doi:10.1021/ja01864a025

Carvalho Lago, C., & Noreña, C. P. Z. (2015). Thermodynamic analysis of sorption isotherms of dehydrated yacon (Smallanthus sonchifolius) bagasse. *Food Bioscience*, *12*, 26–33. https://doi.org/10.1016/j.fbio.2015.07.001

Cheng, X., Ling, P., Iqbal, M. S., Liu, F., Xu, J., & Wang, X. (2023). Water adsorption properties of microalgae powders: Thermodynamic analysis and structural characteristics. *Journal of Stored Products Research*, *101*. https://doi.org/10.1016/j.jspr.2023.102093

Cheng, X., Zhang, M., & Adhikari, B. (2020). Moisture adsorption in water caltrop (Trapa bispinosaRoxb.) pericarps: Thermodynamic properties and glass transition. *Journal of Food Process Engineering*, *43*(8). https://doi.org/10.1111/jfpe.13442

Corrêa, P. C., Baptestini, F. M., Vanegas, J. D. B., Leite, R., Botelho, F. M., & De Oliveira, G. H. H. (2017). Kinetics of water sorption of damaged bean grains: Thermodynamic properties. *Revista Brasileira de Engenharia Agricola e Ambiental*, *21*(8), 556–561. https://doi.org/10.1590/1807-1929/agriambi.v21n8p556-561

Cristina Duarte Marques, R., Resende Oliveira, É., Silva Mendes Coutinho, G., Emannuele Chaves Ribeiro, A., Souza Teixeira, C., Soares Soares Júnior, M., & Caliari, M. (2020). Modeling sorption properties of maize by-products obtained using the Dynamic Dewpoint Isotherm (DDI) method. *Food Bioscience*, *38*. https://doi.org/10.1016/j.fbio.2020.100738

Cuq, B., Rondet, E., & Abecassis, J. (2011). Food powders engineering, between knowhow and science: Constraints, stakes and opportunities. *Powder Technology*, *208*(2), 244–251. https://doi.org/10.1016/j.powtec.2010.08.012

de Souza, S. J. F., Alves, A. I., Vieira, É. N. R., Vieira, J. A. G., Ramos, A. M., & Telis-Romero, J. (2015). Study of thermodynamic water properties and moisture sorption hysteresis of mango skin. *Food Science and Technology (Brazil)*, *35*(1), 157–166. https://doi.org/10.1590/1678-457X.6557

Duarte, Y., Chaux, A., Lopez, N., Largo, E., Ramírez, C., Nuñez, H., Simpson, R., & Vega, O. (2017). Effects of Blanching and Hot Air Drying Conditions on the Physicochemical and Technological Properties of Yellow Passion Fruit (Passiflora edulis Var. Flavicarpa) by-Products. *Journal of Food Process Engineering*, *40*(3). https://doi.org/10.1111/jfpe.12425

Edrisi Sormoli, M., & Langrish, T. A. G. (2016). Spray drying bioactive orange-peel extracts produced by Soxhlet extraction: Use of WPI, antioxidant activity and moisture sorption isotherms. *LWT*, *72*, 1–8. https://doi.org/10.1016/j.lwt.2016.04.033

Fan, K., Chen, L., Wei, X., He, J., & Yan, F. (2015). Moisture Adsorption Isotherms and Thermodynamic Properties of Auricularia auricula. *Journal of Food Processing and Preservation*, *39*(6), 1534–1541. https://doi.org/10.1111/jfpp.12379

García-Pérez, J. V., Cárcel, J. A., Clemente, G., & Mulet, A. (2008). Water sorption isotherms for lemon peel at different temperatures and isosteric heats. *LWT*, *41*(1), 18–25. https://doi.org/10.1016/j.lwt.2007.02.010

Goneli, A. L. D., Corrêa, P. C., de Oliveira, G. H. H., Resende, O., & Mauad, M. (2016). Moisture sorption isotherms of castor beans. Part 1: Mathematical modeling and hysteresis. *Revista Brasileira de Engenharia Agricola e Ambiental*, *20*(8), 751–756. https://doi.org/10.1590/1807-1929/agriambi.v20n8p751-756

Hickey, A. J., & Giovagnoli, S. (2018). *Pharmaceutical Powder and Particles* (R. Zavod, Ed.). American Association of Pharmaceutical Scientist. https://doi.org/https://doi.org/10.1007/978-3-319-91220-2

Kaderides, K., & Goula, A. M. (2017). Development and characterization of a new encapsulating agent from orange juice by-products. *Food Research International*, *100*, 612–622. https://doi.org/10.1016/j.foodres.2017.07.057

Li, X., Han, X., Tao, L., Jiang, P., & Qin, W. (2021). Sorption equilibrium moisture and isosteric heat of Chinese wheat bran products added to rice to increase its dietary fibre content. *Grain and Oil Science and Technology*, *4*(4), 149–164. https://doi.org/10.1016/j.gaost.2021.09.001

Lisboa, H. M., Duarte, M. E., & Cavalcanti-Mata, M. E. (2018). Modeling of food drying processes in industrial spray dryers. *Food and Bioproducts Processing*, *107*, 49–60. https://doi.org/10.1016/j.fbp.2017.09.006

Muzaffar, K., & Kumar, P. (2016). Moisture sorption isotherms and storage study of spray dried tamarind pulp powder. *Powder Technology*, *291*, 322–327. https://doi.org/10.1016/j.powtec.2015.12.046

Osorio-Arias, J., Delgado-Arias, S., Duarte-Correa, Y., Largo-Ávila, E., Montaño, D., Simpson, R., & Vega-Castro, O. (2020). New powder material obtained from spent coffee ground and whey protein; Thermal and morphological analysis. *Materials Chemistry and Physics*, *240*. https://doi.org/10.1016/j.matchemphys.2019.122171

Panesar, R., Kaur, S., & Panesar, P. S. (2015). Production of microbial pigments utilizing agro-industrial waste: A review. In *Current Opinion in Food Science* (Vol. 1, Number 1, pp. 70–76). Elsevier Ltd. https://doi.org/10.1016/j.cofs.2014.12.002

Paul, I. D., & Das, M. (2019). Moisture sorption isotherm and thermodynamic properties of Jamun (Syzygium cumini L.) powder made from jamun pulp and seed. *International Journal of Food Studies*, *8*(1), 111–126. https://doi.org/10.7455/ijfs/8.1.2019.a10

Piercy, E., Verstraete, W., Ellis, P. R., Banks, M., Rockström, J., Smith, P., Witard, O. C., Hallett, J., Hogstrand, C., Knott, G., Karwati, A., Rasoarahona, H. F., Leslie, A., He, Y., & Guo, M. (2022). A sustainable waste-to-protein system to maximise waste resource utilisation for developing food- and feed-grade protein solutions. In *Green Chemistry* (Vol. 25, Number 3, pp. 808–832). Royal Society of Chemistry. https://doi.org/10.1039/d2gc03095k

Polachini, T. C., Betiol, L. F. L., Lopes-Filho, J. F., & Telis-Romero, J. (2016). Water adsorption isotherms and thermodynamic properties of cassava bagasse. *Thermochimica Acta*, *632*, 79–85. https://doi.org/10.1016/j.tca.2016.03.032

Prasantha, R. (2018). Prediction of Moisture Adsorption Characteristics of Dehydrated Fruits Using the GAB Isotherm Model. *Annals of Agricultural and Crop Sciences*, *3*(1). www.austinpublishinggroup.com

Ramírez-Pulido, B., Bas-Bellver, C., Betoret, N., Barrera, C., & Seguí, L. (2021). Valorization of Vegetable Fresh-Processing Residues as Functional Powdered Ingredients. A Review on the Potential Impact of Pretreatments and Drying Methods on Bioactive Compounds and Their Bioaccessibility. In *Frontiers in Sustainable Food Systems* (Vol. 5). Frontiers Media S.A. https://doi.org/10.3389/fsufs.2021.654313

Ray, S., & Boruah, B. (2024). Food Science and Applied Biotechnology Current progress in the valorization of food industrial by-products for the development of functional food products. *Food Science and Applied Biotechnology*, *2024*(2), 2024. https://doi.org/10.30721/fsab2024.v7.i2

Ribeiro-Filho, N., Akepach, P., & Sanchez de Alsina, O. L. (2021). Hygroscopicity and isosteric heat of cashew apple waste, non-fermented and fermented. *Food Bioscience*, *42*. https://doi.org/10.1016/j.fbio.2021.101103

Rifna, E. J., Singh, S. K., Chakraborty, S., & Dwivedi, M. (2019). Effect of thermal and non-thermal techniques for microbial safety in food powder: Recent advances. In *Food Research International* (Vol. 126). Elsevier Ltd. https://doi.org/10.1016/j.foodres.2019.108654

Rosa, D. P., Evangelista, R. R., Borges Machado, A. L., Sanches, M. A. R., & Telis-Romero, J. (2021). Water sorption properties of papaya seeds (Carica papaya L.) formosa variety: An assessment under storage and drying conditions. *LWT*, *138*. https://doi.org/10.1016/j.lwt.2020.110458

Rosa, G. S., Moraes, M. A., & Pinto, L. A. A. (2010). Moisture sorption properties of chitosan. *LWT*, *43*(3), 415–420. https://doi.org/10.1016/j.lwt.2009.09.003

Sahu, C., Patel, S., & Khokhar, D. (2021). Sorption behavior and isosteric heat of maize-millet based protein enriched extruded product. *Heliyon*, *7*(4). https://doi.org/10.1016/j.heliyon.2021.e06742

Santos, D., Lopes da Silva, J. A., & Pintado, M. (2022). Fruit and vegetable by-products' flours as ingredients: A review on production process, health benefits and technological functionalities. In *LWT* (Vol. 154). Academic Press. https://doi.org/10.1016/j.lwt.2021.112707

Sarnavi, H. J., Precoppe, M., García-Triñanes, P., Chapuis, A., Tran, T., Bradley, M. S. A., & Müller, J. (2023). Determining the heat of desorption for cassava products based on data measured by an automated gravimetric moisture sorption system. *Journal of the Science of Food and Agriculture*, *103*(1), 389–399. https://doi.org/10.1002/jsfa.12153

Sawhney, I. K., Sarkar, B. C., Patil, G. R., & Sharma, H. K. (2014). Moisture sorption isotherms and thermodynamic properties of whey protein concentrate powder from buffalo skim milk. *Journal of Food Processing and Preservation*, *38*(4), 1787–1798. https://doi.org/10.1111/jfpp.12148

Silva, E. K., Borges, S. V., da Costa, J. M. G., & Queiroz, F. (2015). Thermodynamic properties, kinetics and adsorption mechanisms of Swiss cheese bioaroma powder. *Powder Technology*, *272*, 181–188. https://doi.org/10.1016/j.powtec.2014.12.002

Simal, S., Femenia, A., Castell-Palou, Á., & Rosselló, C. (2007). Water desorption thermodynamic properties of pineapple. *Journal of Food Engineering*, *80*(4), 1293–1301. https://doi.org/10.1016/j.jfoodeng.2006.10.001

Siqueira-de-Lima, M., Cagnin, C., Borges-Machado, A. L., Ribeiro-Sanches, M. A., Telis-Romero, J., & Resende, O. (2024). Thermodynamic approach on water vapor sorption of Curcuma longa L. flour. *LWT*, *206*. https://doi.org/10.1016/j.lwt.2024.116592

Spada, J. C., Noreña, C. P. Z., Marczak, L. D. F., & Tessaro, I. C. (2013). Water adsorption isotherms of microcapsules with hydrolyzed pinhão (Araucaria angustifolia seeds) starch as wall material. *Journal of Food Engineering*, *114*(1), 64–69. https://doi.org/10.1016/j.jfoodeng.2012.07.019

Tadapaneni, R. K., Yang, R., Carter, B., & Tang, J. (2017). A new method to determine the water activity and the net isosteric heats of sorption for low moisture foods at elevated temperatures. *Food Research International*, *102*, 203–212. https://doi.org/10.1016/j.foodres.2017.09.070

Tao, Y., Wu, Y., Yang, J., Jiang, N., Wang, Q., Chu, D. T., Han, Y., & Zhou, J. (2018). Thermodynamic sorption properties, water plasticizing effect and particle characteristics of blueberry powders produced from juices, fruits and pomaces. *Powder Technology*, *323*, 208–218. https://doi.org/10.1016/j.powtec.2017.09.033

Thys, R. C. S., Noreña, C. P. Z., Marczak, L. D. F., Aires, A. G., & Cladera-Olivera, F. (2010). Adsorption isotherms of pinhão (Araucaria angustifolia seeds) starch and thermodynamic analysis. *Journal of Food Engineering*, *100*(3), 468–473. https://doi.org/10.1016/j.jfoodeng.2010.04.033

Ueda, J. M., Morales, P., Fernández-Ruiz, V., Ferreira, A., Barros, L., Carocho, M., & Heleno, S. A. (2023). Powdered Foods: Structure, Processing, and Challenges: A Review. In *Applied Sciences (Switzerland)* (Vol. 13, Number 22). Multidisciplinary Digital Publishing Institute (MDPI). https://doi.org/10.3390/app132212496

Viganõ, J., Gabas, A. L., & Telis-Romero, J. (2014). Moisture sorption characteristics of pineapple processing waste: Shell and central cylinder. *Journal of Food Process Engineering*, *37*(2), 100–110. https://doi.org/10.1111/jfpe.12064

Villa-Vélez, H. A., Váquiro, H. A., Bon, J., & Telis-Romero, J. (2012). Modelling thermodynamic properties of banana waste by analytical derivation of desorption isotherms. *International Journal of Food Engineering*, *8*(1). https://doi.org/10.1515/1556-3758.2191